Synthesis, Crystal Structures, and Magnetic Properties of a Series of Linear Pentanickel(II) Complexes: $[Ni_5(\mu_5\text{-tpda})_4X_2]$ ($X = Cl^-$, CN^-, N_3^-, NCS^-) and $[Ni_5(\mu_5\text{-tpda})_4(CH_3CN)_2](PF_6)_2$ ($tpda^{2-}$ = the Tripyridyldiamido Dianion)

Chih-Chieh Wang,[†] Wei-Chung Lo,[†] Chin-Chang Chou,[†] Gene-Hsiang Lee,[†] Jin-Ming Chen,[‡] and Shie-Ming Peng*[,†,§]

Department of Chemistry, National Taiwan University, Taipei, Taiwan, ROC, and Synchrotron Radiation Research Center, Hsin Chu, Taiwan, ROC

Received December 29, 1997

The synthesis, crystal structures, and magnetic properties of linear pentanuclear complexes, $[Ni_5(\mu_5\text{-tpda})_4X_2]^{n+}$ [$tpdaH_2$ = tripyridyldiamine, with different axial ligands $X = Cl^-$ (**1**), CN^- (**2**), N_3^- (**3**), and NCS^- (**4**) ($n = 0$) and CH_3CN (**5**) ($n = 2$)], are reported. All of the $[Ni_5(tpda)_4]^{2+}$ moieties are isostructral and involve a Ni_5 linear chain unit with all of the ∠Ni−Ni−Ni being nearly 180°, terminated by the two axial ligands. The pentanuclear linear metal chain is helically wrapped by four *syn*−*syn*−*syn*−*syn* type $tpda^{2-}$ ligands. There are two types of Ni−Ni distances existing in these complexes. The terminal Ni−Ni distances bonded with the axial ligand are longer (2.35−2.40 Å) and affected by various axial ligands. The inner Ni−Ni distances are very short and remain constant (∼2.30 Å). The relationship between terminal Ni−Ni distances and properties of the axial ligands on **1**−**5** will be discussed. Two terminal Ni(II) ions bonded with the axial ligands are in a square-pyramidal (NiN_4X) environment and exhibit long Ni−N bonds (∼2.10 Å) which are consistent with a high-spin Ni(II) configuration. The inner three Ni(II) ions display short Ni−N (∼1.90 Å) bond distances which are consistent with a square-planar (NiN_4), diamagnetic arrangement of a low-spin Ni(II) configuration. All compounds exhibit similar magnetic behavior, indicating an antiferromagnetic interaction of two terminal high-spin Ni(II) ions in these complexes. The XANES (X-ray absorption near-edge absorption spectroscopy) spectra also confirm the existence of the high-spin and low-spin Ni(II) ions in these complexes.

Introduction

The study of metal−metal multiple bonds in transition metal complexes is an interesting and important subject in inorganic chemistry.[1] The characterization of metal−metal bonds in dinuclear metal complexes is well developed and understood.[1−3] The bond orders of M−M bonds derived from theoretical calculations are closely correlated with the M−M bond distances derived from the crystal structures in dinuclear metal complexes.[4−6] Besides dinuclear metal complexes, the extension of three or more bonded metals with a linear metal chain is still in an embryonic state, and only a few cases of M−M-bonded linear trinuclear species (M = Cr, Co, Ni, Cu, Ru, Rh)[7−11] have been reported recently. In our previous report,[12] we synthesized not only a new type of ligand, *N*,*N*′-bis(α-pyridyl)-2,6-diaminopyridine (abbreviated as H_2tpda), but also novel linear pentanuclear complexes, $[Co_5(tpda)_4(NCS)_2]$ and $[Ni_5(tpda)_4Cl_2]$. An unusually short Ni−Ni distance was observed in the $[Ni_5(tpda)_4Cl_2]$ complex. To investigate the magnetic behavior and the structural relationship between Ni−Ni distances and the properties of the axial ligand, a series of $[Ni_5(tpda)_4X_2]$ complexes bonded with various axial ligands, X, were synthesized. The electronic configurations of Ni(II) ions were also characterized in detail by magnetic measurement and X-ray absorption near-edge spectra (XANES).

Experimental Section

Spectroscopic Measurement. The infrared spectra were recorded on a Nicolet Fourier transform IR MAGNA-IR 500 spectrometer in the range of 500−4000 cm^{-1} using the KBr disk technique. UV−visible spectra were recorded on a Hewlett-Packard (HP) 8453

* To whom all correspondence should be addressed.
[†] National Taiwan University.
[‡] Synchrotron Radiation Research Center.
[§] Tel: 886-2-23638305. Fax: 886-2-23636359. E-mail: smpeng@chem35.ch.ntu.edu.tw.

(1) Cotton, F. A.; Walton, R. A. *Multiple Bonds Between Atoms*, 2nd ed.; Clarendon Press: Oxford, U.K., 1993.
(2) Cotton, F. A.; Wilkinson, G. *Advanced Inorganic Chemistry*, 5th ed.; Wiley: New York, 1988; Chapter 23.
(3) *Metal*−*Metal Bonds Clusters in Chemistry and Catalysis*; Plenum: New York, 1989.
(4) Aullon, G.; Alemany, P.; Alvarez, S. *Inorg. Chem.* **1996**, *35*, 5061.
(5) Mota, F.; Novoa, J. J.; Losada, J.; Alvarez, S.; Hoffmann, R.; Silverstre, J. *J. Am. Chem. Soc.* **1993**, *115*, 6216.
(6) Losada, J.; Alvarez, S.; Novoa, J. J.; Mota, F.; Hoffmann, R.; Silverstre, J. *J. Am. Chem. Soc.* **1990**, *112*, 8998.
(7) Yang, E. C.; Cheng, M. C.; Tsai, M. S.; Peng, S. M. *J. Chem. Soc., Chem. Commun.* **1994**, 2377.
(8) Sheu, J. T.; Liu, C. C.; Chao, I.; Wang, C. C.; Peng, S. M. *Chem. Commun.* **1996**, 315.
(9) (a) Wu, L. P.; Field, P.; Morrisey, T.; Murphy, C.; Nagle, P.; Hathaway, B.; Simmons, C.; Thornton, P. *J. Chem. Soc., Dalton Trans.* **1990**, 3835. (b) Pyrka, G. J.; El-Mekki, M.; Pinkerton, A. A. *J. Chem. Soc., Chem. Commun.* **1991**, 84.
(10) Aduldecha, S.; Hathaway, B. *J. Chem. Soc., Dalton Trans.* **1991**, 993.
(11) (a) Cotton, F. A.; Daniels, L. M.; Jordan, G. T., IV. *Chem. Commun.* **1997**, 421. (b) Cotton, F. A.; Daniels, L. M.; Murillo, C. A.; Pascual, I. *J. Am. Chem. Soc.* **1997**, *119*, 10223. (c) Cotton, F. A.; Daniels, L. M.; Jordan, G. T., IV; Murillo, C. A. *J. Am. Chem. Soc.* **1997**, *119*, 10377. (d) Cotton, F. A.; Daniels, L. M.; Murillo, C. A.; Wang, X. *Chem. Commun.* **1998**, 39.
(12) Shieh, S. J.; Chou, C. C.; Lee, G. H.; Wang, C. C.; Peng, S. M. *Angew. Chem., Int. Ed. Engl.* **1997**, *36*, 56.

S0020-1669(97)01608-X CCC: $15.00
Published on Web 07/22/1998

spectrophotometer; maxima are listed in the form λ_{max} (nm) (ϵ (M^{-1} cm^{-1})). The ^1H NMR spectrum of H_2tpda was measured on a Bruker AMX 200 spectrometer.

Preparation of *N*,*N*′-Bis(α-pyridyl)-2,6-diaminopyridine (H_2tpda). The *N*,*N*′-bis(α-pyridyl)-2,6-diaminopyridine (H_2tpda) ligand was synthesized according to the literature.[12] After the accumulation of experimental experience, the yield of H_2tpda was greatly improved from 26% to 60% by 2-chloropyridine instead of 2-bromopyridine.[12] The crude product was recrystallized from 2-propanol, and H_2tpda was obtained. IR (KBr): ν = 3254, 3180 (NH), 1591, 1562, 1541 (C═C) cm^{-1}. MS (FAB) [*m*/*z* (%)]: 264 (100), $[M + 1]^+$. The ^1H NMR in DMSO-d_6 clearly shows 1 singlet (9.37 ppm), 3 doublets (8.20, 7.66, 7.12 ppm), and 3 triplets (7.60, 7.52, 6.84 ppm), which are consistent with the structural assignment.

Preparation of $[Ni_5(\mu_5\text{-tpda})_4(Cl)_2]$ (1). Compound **1** was synthesized according to our previous report.[12] The solid powder were extracted with CH_2Cl_2 and recrystallized from CH_2Cl_2/*n*-hexane solution. Deep purple crystals were obtained (yield 50%). IR (KBr): ν = 1591, 1562, 1541 (C═C) cm^{-1}. MS (FAB) [*m*/*z* (%)]: 1408 (4), $[M]^+$; 1373 (3), $[M - Cl]^+$; 1017 (10), $[Ni_4(\mu_5\text{-tpda})_3]^+$; 698 (10), $[Ni_3(\mu_5\text{-tpda})_2]^+$. The electronic spectrum (CH_2Cl_2 solution, 2×10^{-5} M) shows maxima at λ = 255 nm (ϵ 5.48×10^4 M^{-1} cm^{-1}), 292 nm (ϵ 6.79×10^4 M^{-1} cm^{-1}), 373 nm (ϵ 7.38×10^4 M^{-1} cm^{-1}), 480 nm (ϵ 5.98×10^3 M^{-1} cm^{-1}), 548 nm (ϵ 6.98×10^3 M^{-1} cm^{-1}), and 592 nm (ϵ 7.38×10^3 M^{-1} cm^{-1}). Anal. Calcd for **1**·CH_2Cl_2·$0.5C_6H_{14}$: C, 50.00; H, 3.47; N, 18.22. Found: C, 50.19; H, 3.33; N, 18.53.

Preparation of $[Ni_5(\mu_5\text{-tpda})_4(CN)_2]$ (2). NaCN (27.4 mg, 0.56 mmol) was added to the red-purple solution of $[Ni_5(tpda)_4Cl_2]$ (40 mg, 0.028 mmol) in an Erlemeyer flask (40 mL of THF). The solution was stirred about 5−6 days and then 50 mL of water added to dissolve the unreacted NaCN. The solution was extracted three times by 60 mL of CH_2Cl_2. Na_2SO_4 was added to the organic layer to remove the water. The solution was concentrated, and a red-purple powder was obtained. The powder was recrystallized from a CH_2Cl_2/diethyl ether solution. Deep purple crystals were obtained (yield 45%). IR (KBr): ν = 1591, 1562, 1541 (C═C), 2120 (C≡N) cm^{-1}. MS (FAB) [*m*/*z* (%)]: 1390 (1), $[M]^+$; 1017 (2), $[Ni_4(\mu_5\text{-tpda})_3]^+$. The electronic spectrum (CH_2Cl_2 solution, 2×10^{-5} M) shows maxima at λ = 253 nm (ϵ 5.96×10^4 M^{-1} cm^{-1}), 294 nm (ϵ 7.15×10^4 M^{-1} cm^{-1}), 371 nm (ϵ 8.69×10^4 M^{-1} cm^{-1}), 461 nm (ϵ 6.73×10^3 M^{-1} cm^{-1}), 547 nm (ϵ 8.21×10^3 M^{-1} cm^{-1}), 573 nm (ϵ 8.35×10^3 M^{-1} cm^{-1}). Anal. Calcd for **2**·CH_2Cl_2·$C_4H_{10}O$: C, 51.92; H, 3.64; N, 19.88. Found: C, 52.87; H, 3.79; N, 19.81.

Preparation of $[Ni_5(\mu_5\text{-tpda})_4(N_3)_2]$ (3). NaN_3 (7.3 mg, 0.112 mmol) was added to the red-purple solution of $[Ni_5(tpda)_4Cl_2]$ (40 mg, 0.028 mmol) in an Erlemeyer flask (30 mL of ethanol). Heating about 2−3 h and cooling to room temperature, deep-purple crystals were obtained at the bottom of the flask. The crystals were collected. The solution was extracted by CH_2Cl_2. The organic layer was concentrated, and a red-purple powder was obtained. The powder was recrystallized from CH_2Cl_2/diethyl ether solution, and deep red-purple crystals were obtained (yield 80%). IR (KBr): ν = 1591, 1562, 1541 (C═C), 2045 (azide) cm^{-1}. MS (FAB) [*m*/*z* (%)]: 1422 (1), $[M]^+$; 1017 (2), $[Ni_4(\mu_5\text{-tpda})_3]^+$. The electronic spectrum (CH_2Cl_2 solution, 2×10^{-5} M) shows maxima at λ = 256 nm (ϵ 5.91×10^4 M^{-1} cm^{-1}), 294 nm (ϵ 7.15×10^4 M^{-1} cm^{-1}), 371 nm (ϵ 8.24×10^4 M^{-1} cm^{-1}), 465 nm (ϵ 6.51×10^3 M^{-1} cm^{-1}), 544 nm (ϵ 7.61×10^3 M^{-1} cm^{-1}), 584 nm (ϵ 8.38×10^3 M^{-1} cm^{-1}). Anal. Calcd for **3**·CH_2Cl_2·$C_4H_{10}O$: C, 49.35; H, 3.57; N, 23.02. Found: C, 49.36; H, 3.43; N, 23.27.

Preparation of $[Ni_5(\mu_5\text{-tpda})_4(NCS)_2]$·$4CH_2Cl_2$ (4). $Ni(OAc)_2$·$4H_2O$ (1.488 g, 6 mmol) and $tpdaH_2$ (1.02 g, 4 mmol) were placed in an Erlemeyer flask, to which naphthalene (10 g) was added. The whole mixture was heated (about 180 °C) for 20 min to remove water. Then, *n*-butanol (3 mL) was added to the heated mixture, and heating was continued until the remaining *n*-butanol was completely evaporated. A solution of potassium butoxide (0.88 g, 8 mmol, in 20 mL of *n*-butanol) was added dropwise. Heating was continued until the remaining *n*-butanol was evaporated completely. Then an excess of sodium thiocyanate (1.0 g) was added. After the mixture was cooled, *n*-hexane was added to wash out naphthalene. The remaining solid was extracted with CH_2Cl_2 and recrystallized from CH_2Cl_2/*n*-hexane solution. Deep purple crystals were obtained (yield 50%). IR (KBr): ν= 1591, 1562, 1541 (C═C), 2069 (C≡N) cm^{-1}. MS (FAB) [*m*/*z* (%)]: 1454 (1), $[M]^+$; 1396 (2), $[M - SCN]^+$; 1017 (2), $[Ni_4(\mu_5\text{-tpda})_3]^+$. The electronic spectrum (CH_2Cl_2 solution, 2×10^{-5} M) shows maxima at 256 nm (6.62×10^4 M^{-1} cm^{-1}), 291 nm (8.31×10^4 M^{-1} cm^{-1}), 373 nm (9.49×10^4 M^{-1} cm^{-1}), 465 nm (7.29×10^3 M^{-1} cm^{-1}), 546 nm (8.65×10^3 M^{-1} cm^{-1}), 585 nm (9.54×10^3 M^{-1} cm^{-1}). Anal. Calcd for **4**·C_6H_{14}: C, 53.00; H, 3.79; N, 19.99. Found: C, 53.02; H, 3.92; N, 19.57.

Preparation of $[Ni_5(\mu_5\text{-tpda})_4(CH_3CN)_2](PF_6)_2$ (5). $[Ni_5(tpda)_4Cl_2]$ (40 mg, 0.028 mmol) was placed into an Erlemeyer flask containing 30 mL of CH_2Cl_2 to give a dark purple solution. The solution was stirred, and then $AgPF_6$ (14.86 mg, 0.059 mmol) and 2 mL of CH_3CN were added to the solution in the Erlemeyer flask. After the mixture was stirred for about 30 min, a white powder (AgCl) was precipitated. The solution was filtered to remove the AgCl. The solution was concentrated to 5 mL and diffused from CH_2Cl_2/diethyl ether solution. Deep purple crystals were obtained (yield 58%). IR (KBr): ν = 1591, 1562, 1541 (C═C), 2045 (C≡N), 842 (PF_6) cm^{-1}. MS (FAB) [*m*/*z* (%)]: 1362 (1), $[M]^+$. The electronic spectrum (CH_2Cl_2 solution, 2×10^{-5} M) shows maxima at λ = 253 nm (ϵ 5.11×10^4 M^{-1} cm^{-1}), 288 nm (ϵ 6.43×10^4 M^{-1} cm^{-1}), 372 nm (ϵ 7.01×10^4 M^{-1} cm^{-1}), 552 nm (ϵ 5.98×10^3 M^{-1} cm^{-1}), 597 nm (ϵ 5.88×10^3 M^{-1} cm^{-1}). Anal. Calcd for **5**·$3CH_2Cl_2$: C, 40.95; H, 2.87; N, 15.68. Found: C, 40.69; H, 2.97; N, 15.92.

Crystallographic Procedures. Suitable single crystals of **1**−**5** were selected under a microscope and mounted in glass capillaries. All the measurements were made on a Nonius CAD4 diffractometer with

Table 1. Crystal and Refinement Data for Compounds **1**−**5**

	compd		
	1	**2**	**3**
formula	$Ni_5Cl_{10}N_{20}C_{64}H_{52}$	$Ni_5Cl_2N_{22}C_{63}H_{44}$	$Ni_5N_{26}C_{60}H_{44}$
fw	1749.31	1473.63	1422.72
cryst system	monoclinic	tetragonal	monoclinic
space group	$P2_1/n$	$I4/m$	$P2_1/n$
color	dark purple	dark purple	dark purple
cryst size	$0.25 \times 0.4 \times 0.5$	$0.1 \times 0.4 \times 0.5$	$0.2 \times 0.3 \times 0.35$
a (Å)	13.416(3)	10.606(3)	10.492(2)
b (Å)	16.894(3)		18.475(4)
c (Å)	15.807(4)	27.065(5)	14.738(5)
α (deg)			
β (deg)	92.54(3)		93.47(3)
γ (deg)			
V (Å^3)	3579(1)	3044(1)	2851(1)
Z	2	2	2
ρ_{calcd} (g·cm^{-3})	1.623	1.608	1.657
μ (cm^{-1})	14.211	16.755	16.955
$R(F_o)$; $R_w(F_o)^a$	0.072; 0.071	0.050; 0.042	0.054; 0.049
GOF	2.75	2.02	1.77

	compd	
	4	**5**
formula	$Ni_5Cl_8S_2N_{22}C_{66}H_{52}$	$Ni_5N_{26}C_{72}H_{62}P_2F_{12}$
fw	1794.56	1874.91
cryst system	triclinic	triclinic
space group	$P\bar{1}$	$P\bar{1}$
color	dark purple	dark purple
cryst size (mm)	$0.3 \times 0.6 \times 0.6$	$0.2 \times 0.2 \times 0.4$
a (Å)	12.042(8)	11.424(6)
b (Å)	13.985(5)	12.479(3)
c (Å)	22.894(7)	14.290(3)
α (deg)	90.33(3)	97.04(3)
β (deg)	89.86(4)	92.34(4)
γ (deg)	103.80(4)	106.83(4)
V (Å^3)	3744(3)	1929(1)
Z	2	1
ρ_{calcd} (g·cm^{-3})	1.592	1.614
μ (cm^{-1})	14.908	13.247
$R(F_o)$; $R_w(F_o)^a$	0.058; 0.058	0.058; 0.050
GOF	1.57	2.00

^{a} $R(F_o) = \sum|F_o - F_c|/\sum|F_o|$; $R_w(F_o) = (\sum w|F_o - F_c|^2/\sum w|F_o|^2)^{1/2}$.

graphite-monochromated Mo Kα radiation ($\lambda = 0.7107$ Å). The data were collected at room temperature using the $\omega-2\theta$ scan technique to maximum 2θ of 45° for **2**, **4**, and **5** and of 50° for **1** and **3**. The cell parameters were determined using 25 reflections in the 2θ ranges of $12.16° \le 2\theta \le 28.60°$ for **1**, $15.34° \le 2\theta \le 20.20°$ for **2**, $17.00° \le 2\theta \le 23.44°$ for **3**, $15.00° \le 2\theta \le 24.10°$ for **4**, and $14.80° \le 2\theta \le 24.24°$ for **5**. Three intensity-control reflections for every complex were monitored every 3600 s during the data collection. The intensity data were corrected for Lorentz and polarization effects, and refinement was performed using the counting statistics weighting scheme. An empirical absorption correction based on three azimuthal scans was also applied. The structures were solved using direct methods and difference Fourier techniques and refined by least-squares analysis. The non-hydrogen atoms were refined anisotropically, and the hydrogen atoms were included in an idealized geometry but not refined. The detailed data collection and refinement parameters of these complexes are summarized in Table 1. Other crystallographic data are given as Supporting Information. All calculations were carried out with the NRCVAX[13] program on the VAX Alpha station.

Magnetic Susceptibility Measurement. Experimental Method. The temperature-dependent magnetic susceptibility was measured on the SQUID system with 10 000 G external magnetic field. Molar magnetic susceptibility was recorded every 5 K in the range of 5−300 K.

Magnetic Simulation. The Ni(II) ions with d^8 electrons are divided into two states, high-spin $S = 1$ and low-spin $S = 0$ configurations. According to the structural analysis of $[Ni_5(tpda)_4X_2]$, the three inner Ni(II) ions are in low-spin state and two terminal Ni(II) ions are in high-spin state. If only the interactions between metal atoms are taken into account, the Hamiltonian of the spin−spin exchange interaction for those complexes can be written as follows:[14]

$$H = -2\sum_{j>i=1}^{5} J_{ij}S_i\cdot S_j = -(2\sum_{j>i=1}^{4} J_{ij}S_i\cdot S_j + 2\sum_{i=2}^{4} J_{i5}S_i\cdot S_5 + 2J_{15}S_1\cdot S_5) \quad (1)$$

The differential equation of eigenvalue $E(S_T)$ is then

$$E(S_T) = -\sum_{j>i=1}^{4}(J_{ij} - J_{15})[S_{ij}(S_{ij}+1) - S_i(S_i+1) - S_j(S_j+1)] - \sum_{i=2}^{4}(J_{i5} - J_{15})[S_{i5}(S_{i5}+1) - S_i(S_i+1) - S_5(S_5+1)] - J_{15}S_T(S_T+1) + J_{15}\sum_{i=1}^{5} S_i(S_i+1) \quad (2)$$

When the spins of five Ni(II) ions are assumed to be $S_1 = S_5 = 1$ and $S_2 = S_3 = S_4 = 0$ and the coupling constants are constraint as $J_{12} = J_{45}$, $J_{23} = J_{34}$, and $J_{13} = J_{35}$ according to the symmetry, then eq 2 can then be simplified to

$$E(S_T) = -J_{13}S_T(S_T+1) + S_{15}(S_{15}+1)(J_{13} - J_{15}) + 4J_{23} + 2J_{15} - 2J_{13} \quad (3)$$

Considering the Boltzmann distributions of molecules on each energy level (E_i), the molar magnetic susceptibility χ_M can be described by the following equation:

$$\chi_M = (Ng^2\beta^2/3kT)(\sum_{S_T} S_T(S_T+1)(2S_T+1)e^{-E(S_T)/kT})/(\sum_{S_T}(2S_T+1)e^{-E(S_T)/kT}) \quad (4)$$

Using the simple vectorial coupling rule, (S_T;S') is the combination of the sum of spin S_T and partial spin value S'. These values are (2;2),(1;1), and (0;0), respectively. The theoretical molar magnetic susceptibility χ_M of $[Ni_5(dpa)_4X_2]$ can be derived by the equation

$$\chi_M = C(2e^{2x} + 10e^{5x})/(1 + 3e^{2x} + 5e^{6x}) \quad (5)$$

where

$C = Ng^2\beta^2/kT$ $\quad x = J_{15}/kT$
$N = 6.022 \times 10^{23}$ $\quad g$: g-factor
β: Bohr magneton $\quad k$ (Boltzmann): 0.695 $cm^{-1}K^{-1}$
T: abs temp (K) $\quad J_{15}$: coupling const between Ni(1) and Ni(5)

Since there still exists some magnetic moment even at low temperature, it is believed that the sample contained some paramagnetic impurities; therefore the corrected χ_M can be written as

$$\chi_M = (1-P)C'(2e^{2x} + 10e^{5x})/(1 + 3e^{2x} + 5e^{6x}) + P(2Ng^2\beta^2/3kT) + N_\alpha \quad (6)$$

$$C' = Ng^2\beta^2/k(T - \Theta)$$

Θ: Weiss temperature (or Weiss constant)

P: relative content for paramagnetic impurity where spin state $S = 1$ is assumed

N_α: temperature-independent paramagnetism, TIP

Ni(II) $L_{II,III}$-Edge X-ray Absorption Measurement. The Ni $L_{II,III}$-edge X-ray absorption spectra of $[Ni_3(dpa)_4(NCS)_2]$, $[Ni_5(tpda)_4(NCS)_2]$, and a model high-spin compound, $[Ni(NH_3)_6]^{2+}$, were recorded using the high-energy spherical grating monochromator (HSGM) beamline at the Synchrotron Radiation Research Center (SRRC) in Taiwan. A refocusing mirror produced an $\sim 1 \times 3$ mm^2 beam spot on the samples. The energy resolution of the monochromator was set to ~0.35 eV at the Ni 2p edge. The measurement chamber was maintained at a vacuum of less than 2×10^{-9} mbar. The Ni $L_{II,III}$-edge X-ray absorption spectra of the samples were recorded using the total electron yield mode. The incident beam intensity (I_0) was measured simultaneously from a Au-coated grid located between the sample and monochromator. All the absorption spectra were normalized to I_0. The photo energies were calibrated using the Ni L_{III}-edge absorption peak at 852.7 eV of the Ni compound. Comparison of data from several scans showed no photoreduction or radiation damage in all these compounds.

Results and Discussions

Synthesis of H_2tpda, All *Anti* Form and All *Syn* Form Complexes. No matter what the ratio use for 2-chloropyridine and 2,6-diaminopyridine when they were added together, H_2-dpda was always coexisted with the major product of H_2tpda.

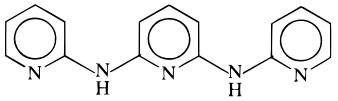

H_2tpda

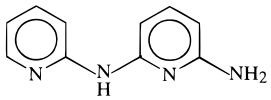

H_2dpda

The way to separate H_2tpda and H_2dpda is recrystallizing the mixtures in 2-propanol solution, where H_2dpda is soluble in 2-propanol and H_2tpda is only slightly soluble. The IR spectra for both compounds are very similar with 3254 and 3180 cm^{-1} for ν(NH) and 1200−1600 cm^{-1} for ν(C−C) of the pyridine ring, but the peak of 3442 cm^{-1} for $\nu(NH_2)$ can only be observed in H_2dpda. The MS (FAB) indicates m/z 263 for H_2tpda and m/z 187 for H_2dpda.

The coordination chemistry of the H_2tpda ligand can be divided into two types of conformations, the *anti−anti−anti−anti* form **I** and the *syn−syn−syn−syn* form **II**.

(13) Gabe, E. J.; Le Page Y.; Charland, J.-P.; Lee, F. L.; White, P. S. *J. Appl. Crystallogr.* **1989**, *22*, 384.
(14) (a) Kambe, K. *J. Phys. Soc.* **1950**, *5*, 48. (b) Sinn, E. *Coord. Chem. Rev.* **1970**, *5*, 313.

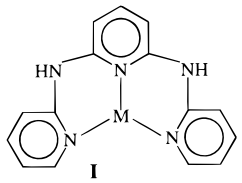

I

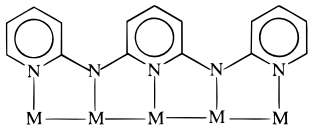

II

The metal complexes as form **I** can be synthesized by a conventional method with equimolar amounts of $MCl_2 \cdot nH_2O$ or $M(BF_4)_2 \cdot nH_2O$ with H_2tpda. The H_2tpda acts as a tridentate ligand and coordinates to metal ions through the nitrogen atoms of pyridine moieties. The metal ions can bind either one H_2-tpda ligand to form $M(tpdaH_2)$ (M = Co, Zn, Cu) or two H_2-tpda ligands to form $M(tpdaH_2)_2$ (M = Fe, Cu, Ni) complexes.[12,15] None of all *syn* form pentanickel complexes of **II**, however, can be obtained by a conventional method. Two ways are found to synthesize the $[Ni_5(tpda)_4X_2]$ complexes. The first one is a special synthetic method in which the *t*-BuOK is used to deprotonate the H_2tpda ligand under heating with naphthalene. $tpda^{2-}$ then acts as a pentadentate ligand to bind with five Ni atoms. The other method involves the axial ligand replacement in which $AgPF_6$ is used to pull away the Cl^- of $[Ni_5(tpda)_4Cl_2]$, after which various ligands can be added to the axial positions. The synthetic procedures of $[Ni_5(tpda)_4X_2]$ are described in Scheme 1.

All of the infrared spectra of the $[Ni_5(tpda)_4X_2]$ compounds are similar except the axial ligand's vibrational mode. The N−H stretching bands of H_2tpda in the 3254 cm^{-1} region are completely absent, and C−C vibrational modes of the pyridine ring are shown in the range of 1200−1600 cm^{-1}. The MS (FAB) of parent peaks of compounds **1**−**5** are observed at *m*/*z* 1390, 1422, 1454, 1362, and 1408, respectively, and consistent with the simulated patterns.

Structural Results. The center Ni^{II} ion is located at the crystallographic center of inversion in compounds **1**, **2**, and **5** and at the 4-fold and mirror symmetries (4/*m*) in compound **3**, respectively. The atomic positions of these four compounds are averaged, because the right-turn and left-turn helical complexes are disordered. One of the helical forms of compound **1** is shown in Figure 1. Other figures of crystal structures for compounds **2**, **3**, and **5** are given as Supporting Information. Eight nitrogen atoms from the amido group that are coordinated to nickel ion (N2, occupancy factor 0.5) and the α-carbon atoms of the pyridyl groups have high anisotropic thermal parameters. The space group of compound **4** is $P\bar{1}$ with a whole complex and four CH_2Cl_2 molecules in the asymmetric unit. The disordered problem is not observed in this structure. The geometric structure of **4** is shown in Figure 2. Comparing the anisotropic thermal ellipsoids of the amido and pyridyl groups between Figures 1 and 2, the anisotropic thermal ellipsoids of the amido and pyridyl groups in compound **4** are more regular than those of the amido and pyridyl groups in compound **1**. The detailed bond distances and bond angles of these compounds are listed in the Supporting Information.

The $[Ni_5(tpda)_4]^{2+}$ fragments of compounds **2**−**5** are isostructral with those of $[Ni_5(tpda)_4Cl_2]$ (**1**), as we described in the previous report.[12] The pentanuclear linear metal chain is helically wrapped by four *syn*−*syn*−*syn*−*syn* type $tpda^{2-}$ ligands. All of the nickel ions and two axial ligands are nearly collinear. Two types of Ni−Ni distances, named terminal (connected with axial ligand) and inner Ni−Ni bonds, exist in these compounds. Both of them are very short. The former

(15) Yang, M. H.; Lin, T. W.; Chou, C. C.; Lee, H. C.; Chang, H. C.; Lee, G. H.; Leung, M. K.; Peng, S. M. *Chem. Commun.* **1997**, 2279.

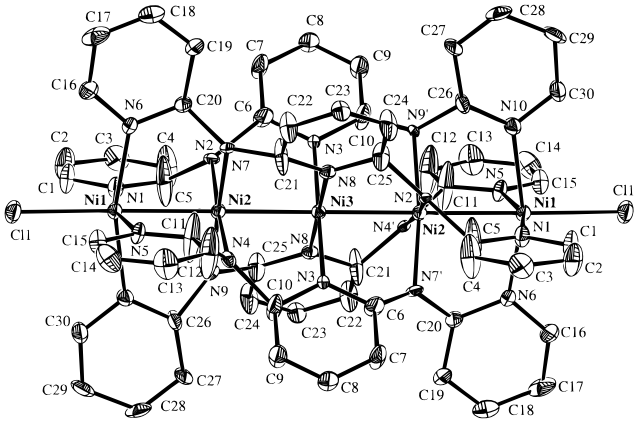

Figure 1. Crystal structure of $[Ni_5(\mu_5\text{-tpda})_4Cl_2]$ (**1**). Atoms are shown as 20% vibrational thermal ellipsoids.

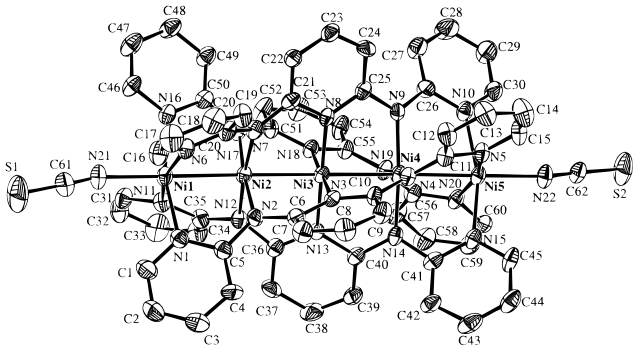

Figure 2. Crystal structure of $[Ni_5(\mu_5\text{-tpda})_4(NCS)_2]$ (**4**). Atoms are shown as 20% vibrational thermal ellipsoids.

Scheme 1. Synthetic Procedures for $[Ni_5(tpda)_4X_2]$.

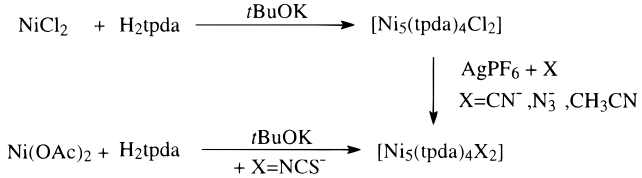

Table 2. Comparisons of Selected Bond Distances (Å) for $[M_5(tpda)_4X_2]$ Complexes

M	X	Ni1−Ni2	Ni2−Ni3	Ni1−N_{av}	Ni2−N_{av}	Ni3−N_{av}
Ni	Cl^- (**1**)[12]	2.385(2)	2.306(1)	2.111(9)	1.90(2)	1.904(8)
Ni	CN^- (**2**)	2.400(3)	2.296(2)	2.094(7)	1.91(1)	1.897(8)
Ni	N_3^- (**3**)	2.379(2)	2.298(2)	2.082(8)	1.90(1)	1.901(7)
Ni	SCN^- (**4**)	2.367(2)	2.298(2)	2.09(1)	1.89(1)	1.897(8)
		2.371(2)	2.294(2)	2.09(1)	1.89(1)	
Ni	CH_3CN (**5**)	2.346(3)	2.291(2)	2.101(9)	1.90(2)	1.898(9)
Co[12]	SCN^-	2.277(2)	2.232(2)	1.97(1)	1.90(1)	1.93(1)
		2.274(2)	2.229(2)	1.97(1)	1.90(1)	

one is longer (2.340−2.400 Å) and influenced by the axial ligands. The comparisons of the terminal M−M bond distances among various axial ligands (compounds **1**−**5**) are listed in Table 2. The terminal Ni−Ni distance is the longest one (2.400-(3) Å) when the axial ligand is a strong *σ*-donor ligand, CN^-, but the terminal Ni−Ni distance is the shortest one (2.346(3) Å) when the axial ligand is a solvent-coordinated ligand, CH_3-CN. The terminal Ni−Ni distances with the axial ligands, X = N_3^-, NCS^-, and Cl^-, are 2.379(2), 2.369(2), and 2.385(3) Å, respectively. In addition to the properties of the axial ligand, the steric repulsion between the axial ligand and the Ni atom also affects the terminal Ni−Ni distance. If the terminal Ni−Ni bond distances are compared among three N-connected axial ligands (X = N_3^- (**3**), SCN^- (**4**), and CH_3CN (**5**)), the terminal

Ni−Ni bond distances decrease in the order of 2.379(2) Å (**3**) > 2.369(2) Å (**4**) > 2.346(3) Å (**5**) as the ∠Ni−N−N (or ∠Ni−N−C) increase in the order of 136.8(9)° (**3**) < 160(1)° (**4**) < 174.4(9)° (**5**). These results reveal that the σ-donor ability of the axial ligand and the linearity between Ni and the axial ligand both affect the terminal Ni−Ni distance. The weaker the axial ligand's σ-donor ability and the better the linearity between Ni and the axial ligand, the shorter the terminal Ni−Ni distance. These trends are observed not only on the pentanuclear linear metal chain complexes but also on the trinuclear ones.[16] The inner Ni−Ni distance is the shortest one (∼2.300 Å) that we have found in the literature[17−19] and remained constant no matter what the axial ligand is. If we compare the M−M bonds with different metal centers, both of the Ni−Ni distances (2.369(2), 2.300(2) Å) found in $[Ni_5(tpda)_4(NCS)_2]$ are longer than those (2.276(2), 2.231(2) Å) in $[Co_5(tpda)_4(NCS)_2]$. This result can be explained from molecular orbital analysis and will be discussed in the theoretical part. If the Ni−Ni bond separations are ignored, the three inner Ni ions in these complexes are all four-coordinated, square planar conformations. All of the mean Ni−N distances of 1.89−1.90 Å are short, consistent with the Ni−N distance, ca. 1.90 Å, usually found in the low-spin (S = 0) square planar Ni(II) configuration system.[20] The terminal Ni(II) ions are in a square pyramidal environment, to give a NiN_4X chromophore. The basal plane consists of four independent $tdpa^{2-}$ ligands, and the mean Ni−N distances are about 2.10 Å consistent with a high-spin Ni(II) configuration for these terminal Ni(II) ions.[21] Two terminal Ni atoms are displaced out of the N_4 planes, ca. 0.284(5), 0.286(2), 0.265(4), 0.271(5), and 0.231(5) Å for compounds **1**−**5**, respectively.

The $tpda^{2-}$ ligands act as pentadentate nitrogen chelating ligands. No unusual bond lengths or angles are found in the $tpda^{2-}$ ligand. Each pentadentate ligand is nonplanar, with an average dihedral angle among three pyridine rings of approximately 45° and results in a spiral structure for these pentanuclear complexes. The molecule structure of the $[Ni_5(tpda)_4]^{2+}$ fragment viewed down the linear metal chain is shown in Figure 3 and gives a better view of this spiral structure.

Molecular Orbital Calculations. To analyze the bonding features of five centered M−M−M−M−M bonds and compare the M−M bond order with different metal centers (Co, Ni), a simple molecular orbital calculation, namely the extended Hückel molecular orbital method (EHMO), was chosen to apply to such a large system. The EHMO is performed using the program ICON.[22] The basis functions of S, C, N, and H are taken from the default values of the program. The basis functions of Co and Ni are taken from the literature[23] [Co: H_{ii}(4s) = −9.21 eV, ζ = 2.0; H_{ii}(4p) = −5.29 eV, ζ = 2.0; H_{ii}(3d) = −13.18 eV, ζ_1 = 5.55, C_1 = 0.568, ζ_2 = 2.10, C_2 = 0.606. Ni: H_{ii}(4s) = −10.95 eV, ζ = 2.1; H_{ii}(4p) = −6.27 eV, ζ = 2.1; H_{ii}(3d) = −14.2 eV, ζ_1 = 5.75, C_1 = 0.5798, ζ_2 = 2.30, C_2 = 0.5782]. The atomic coordinates are derived directly from the X-ray diffraction data of $[Co_5(tpda)_4(NCS)_2]$[12] and $[Ni_5(tpda)_4(NCS)_2]$ for the purpose of avoiding the disordered problem. Figure 4 presents only the molecular orbitals related to five centered Co−Co−Co−Co−Co bonds, which provide the qualitative bonding description of the M−M−M−M−M bonds. The relative energy levels of the Co−Co−Co−Co−Co bonds in Figure 4 consist of five σ bonds (linear combination of five M(sd_{z^2}) orbitals), 10 π bonds (linear combination of five M(d_{xz}, d_{yz}) orbitals), and five nonbonding orbitals (lone pair of M(d_{xy} or $d_{x^2-y^2}$ orbital)). No or weak δ bonds are found because of the spiral structure of the $tpda^{2-}$ ligand. The molecular orbital diagram of the Ni−Ni−Ni−Ni−Ni bonds is very similar to that in Figure 4 as shown in

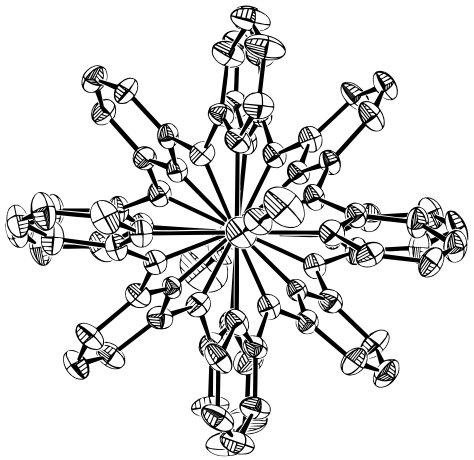

Figure 3. Helical view of $[Ni_5(\mu_5\text{-}tpda)_4(NCS)_2]$ (**4**) with the molecule looking down the Ni_5 axis. Atoms are shown as 20% vibrational thermal ellipsoids.

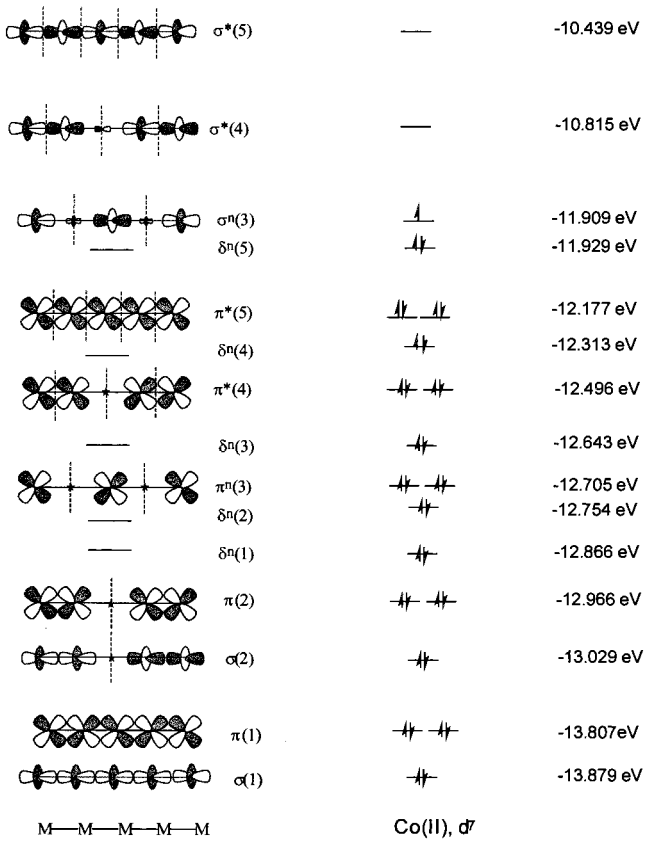

Figure 4. Molecular orbital diagram of the linear five Co_5 system for $[Co_5(tpda)_4(NCS)_2]$.

(16) Lo, W. C. Ph.D. Thesis, National Taiwan University, 1997.
(17) Jarchow, O.; Schultz, H.; Nast, R. *Angew. Chem.* **1970**, *84*, 43; *Angew. Chem., Int. Ed. Engl.* **1970**, *9*, 71. Ni−Ni = 2.32 Å in $[Ni^{I}_2(CN)_6]^{4-}$.
(18) Sacconi, L.; Mealli, C.; Gatteschi, D. *Inorg. Chem.* **1974**, *13*, 1895. Ni−Ni = 2.42 Å in $[Ni^{1.5}_2(napy)_4Br_2]^{+}$, where napy = 1,8-naphthyridine.
(19) Corbett, M.; Hoskins, B. *Chem. Commun.* **1969**, 1602. Ni−Ni = 2.38 Å in $[Ni^{II}_2(PhN_3Ph)_4]$, where PhN_3Ph = diphenyltriazenato.
(20) Sacconi, L.; Mani, F.; Bencini. In *Comprehensive Coordination Chemistry*; Wilkinson, G., Gillard, R. D., McCleverty, J. A., Eds.; Pergamon: Oxford, U.K., 1987; Vol. 5, section 50.
(21) Long, G. J.; Schlemper, E. O. *Inorg. Chem.* **1974**, *13*, 279.
(22) Howell, J.; Rossl, A.; Wallace, D.; Haraki, K.; Hoffmann, R. ICON Program for Extended Huckel molecular orbital calculations. *Quantum chemistry program exchange*; University of Indiana: Bloomington, IN, 1977.

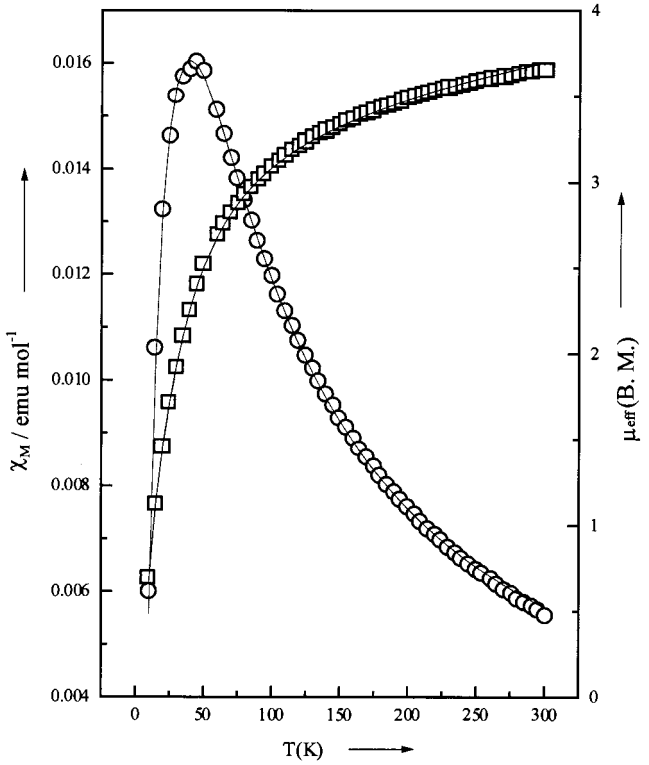

Figure 5. Magnetic data for $[Ni_5(\mu_5\text{-tpda})_4(CN)_2]$ (**2**). The solid line represents the results of theoretical simulation. ○ indicates the observed χ_M, and □, the observed μ_{eff}.

Supporting Information. A total of 35 electrons of Co^{II} and 40 electrons of Ni^{II} are to be filled in these orbitals. According to the orbital analysis of energy diagram, there are 2.5 net bond paired electrons ($\sigma(1)^2$, $\sigma(2)^2$, $\sigma^n(3)^1$) in the Co−Co−Co−Co−Co bonds but no net bond paired electrons are in the Ni−Ni−Ni−Ni−Ni bonds. The bond order of Ni−Ni is obviously zero. The overlap populations among metals are [0.20, 0.12, 0.12, 0.20] for [Co−Co−Co−Co−Co] and [0.08, 0.08, 0.08, 0.08] for [Ni−Ni−Ni−Ni−Ni]. Obviously, the Co−Co bond strength is stronger than the Ni−Ni bond strength. The Co−Co bond distances should be shorter than the Ni−Ni bond distances. This result is comparable with the structural analysis.

Magnetic Properties of $[Ni_5(tpda)_4X_2]$. The experimental curves of the molar magnetic susceptibility χ_M (○) and effective magnetic moment (μ_{eff}) (□) with respect to temperature (T) for compound **2** are displayed in Figure 5. The experimental curve is almost the same as the one obtained from magnetic simulation (solid line). That means the electronic configurations derived from structural analyses are in good agreement with the experimental magnetic measurements, with three inner Ni(II) ions being in a low-spin ($S = 0$) state and two terminal Ni(II) ions being in high-spin ($S = 1$) states. Other magnetic curves of compounds **3**, **4**, and **5** are very similar to that of compound **2**. The observed room-temperature magnetic moment μ_{eff} of compounds **2**−**5** are 2.62, 2.72, 2.79, and 2.69 per paramagnetic nickel(II) ions (3.70, 3.85, 3.94, 3.81 per pentanuclear Ni complexes), respectively, a little less than the spin-only value of 2.83 for the free nickel(II) ion. The lower value of observed magnetic moment also shows that the square pyramidal environments of two terminal nickel(II) ions involve high-spin species.[20] The coupling constants (J_{15}) obtained from theoretical simulations for various axial ligands are listed in Table 3. The J value for compound **1** is corrected from -14.6 cm^{-1} in our previously report[12] to -8.27 cm^{-1} by including the relative content for paramagnetic impurity (P) term in eq 6. The negative J values

Table 3. Simulation Data for $[Ni_5(tpda)_4X_2]$ Complexes

X	J_{15} (cm^{-1})	Ni- - -Ni* [a]	Θ	TIP	P	R
Cl^- (**1**)	−8.27	9.382	−44.47	0	0.027 87	0.001 84
CN^- (**2**)	−6.40	9.392	−45.57	0	0.001 77	0.000 74
N_3^- (**3**)	−8.17	9.354	−32.65	0	0	0.003 42
SCN^- (**4**)	−9.24	9.330	−36.72	0	0.107 91	0.002 38
CH_3CN (**5**)	−9.70	9.274	−63.64	0.00132	0.156 23	0.001 37

[a] Distance between two terminal Ni(II) ions (Å).

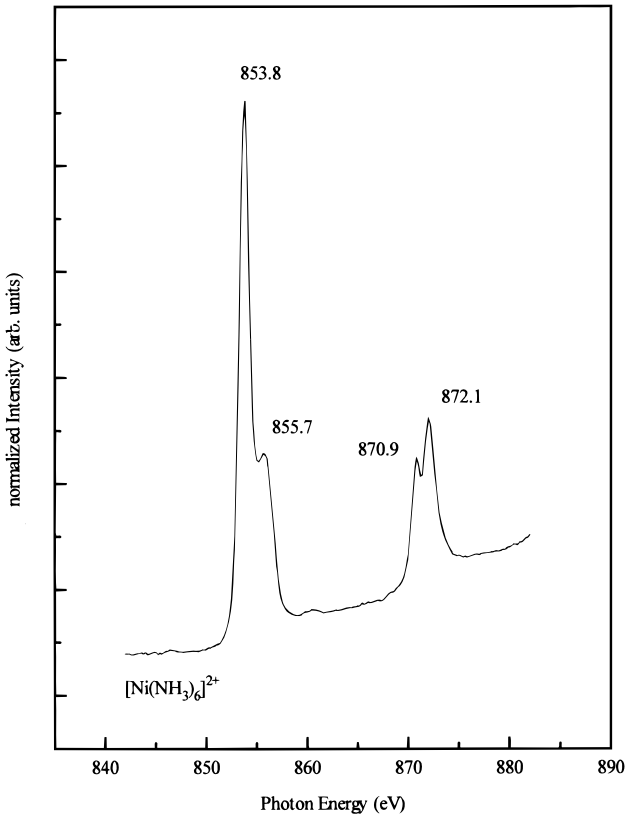

Figure 6. Ni $L_{II,III}$ X-ray absorption spectra of $[Ni(NH_3)_6]^{2+}$.

in Table 3 reveal the antiferromagnetic interactions between two terminal high-spin nickel ions. These interactions are 1 order of magnitude smaller than those of similar trinuclear Ni(II) complexes.[24] This result reveals that the antiferromagnetic interaction is correlated with the distance between two terminal Ni(II) ions. In Table 3, the $|J|$ value is the largest (9.7 cm^{-1}) when two terminal Ni- - -Ni distances is shortest (9.274 Å), but the $|J|$ value is the smallest (6.40 cm^{-1}) when two terminal Ni- - -Ni distances are the longest (9.392 Å).

X-ray Near-Edge Absorption Spectra. The $L_{II,III}$ edges are sensitive to oxidation state, spin state, and ligand field changes of the absorbing 3d transition metal.[25−28] It has been experimentally shown[26] that significant differences in Ni $L_{II,III}$-edge

(23) Summerville, R. H.; Hoffmann, R. *J. Am. Chem. Soc.* **1976**, *98*, 7240.
(24) Unpublished work. The coupling constants (J_{13}) of $[Ni_3(dpa)_4X_2]$ are −99 (X = Cl$^-$), −101 (X = N_3^-), −123 (X = NCS^-), and −167 cm^{-1} (X = C_3H_7CN).
(25) Thole, B. T.; Crwan, R. D.; Sawatzky, G. A.; Fink, J.; Fuggle, J. C. *Phys. Rev. B* **1985**, *31*, 6856.
(26) van der Laan, G.; Kirkwood, I. W. *J. Phys.*: *Condens Matter*. **1992**, *4*, 4189.
(27) Cramer, S. P.; de Groot, F. M. F.; Ma, Y.; Chen, C. T.; Sette, F.; Kipke, C. A.; Eichhorn, D. M.; Chan, M. K.; Armstrong, W. H.; Libby, E.; Christou, G.; Brooker, S.; McKee, V.; Mullins, O. C.; Fuggle, J. C. *J. Am. Chem. Soc.* **1991**, *113*, 7937−7940.
(28) Briois, V.; Cartier dit Moulin, C.; Sainctavit, P.; Brouder, C.; Flank, A. M. *J. Am. Chem. Soc.* **1995**, *117*, 1019.

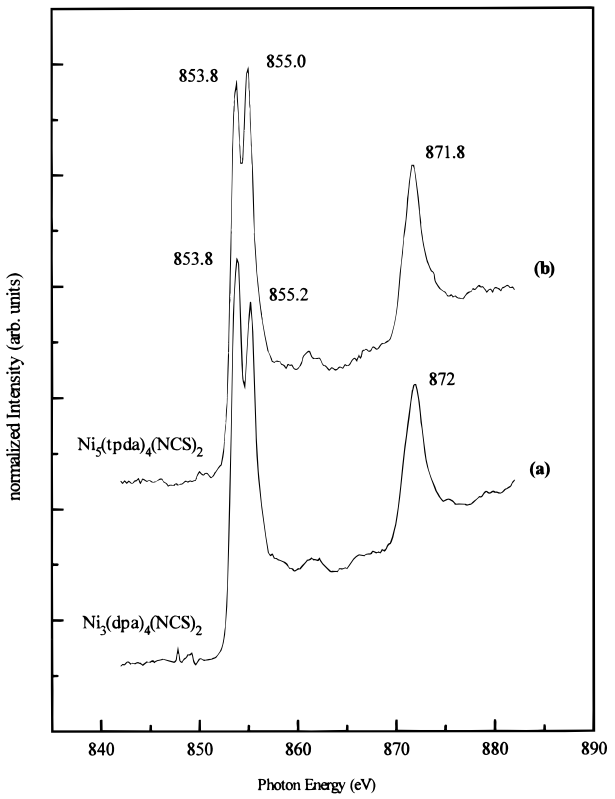

Figure 7. (a) Ni $L_{II,III}$ X-ray absorption spectra of $[Ni_3(\mu_3\text{-dpa})_4(SCN)_2]$. (b) Ni $L_{II,III}$ X-ray absorption spectra of $[Ni_5(\mu_5\text{-tpda})_4(SCN)_2]$.

absorption spectra were observed between triplet high-spin and singlet low-spin Ni^{II} compounds.[29] The L_{III} edge of the low-spin compound is at higher energy than that of the high-spin compound.[29,30] The Ni $L_{II,III}$-edge absorption spectrum of the model high-spin O_h $[Ni(NH_3)_6]^{2+}$ complex is shown in Figure 6, which reveals one strong peak (853.8 eV) with a distinctive shoulder (855.7 eV) at the L_{III} edge and two peaks (870.9 and 872.1 eV) at the L_{II} edge. In Figure 7a,b, we show the Ni $L_{II,III}$-edge absorption spectra of trinuclear Ni complex $[Ni_3(dpa)_4(NCS)_2]$ ($dpa^- =$ dipyridylamido anion) and pentanuclear Ni complex $[Ni_5(tpda)_4(NCS)_2]$. In both spectra we find two strong peaks, 855.2 and 853.8 eV, at the L_{III} edge and one strong peak, 872 eV, at the L_{II} edge. If we compare the Ni L_{III} edge in these three spectra shown in Figures 6 and 7, the peak at 855.2 eV is certainly not from the high-spin case. This result may indicate that two types of Ni(II) spin configurations, i.e., low-spin and high-spin, coexist in $[Ni_3(dpa)_4(NCS)_2]$ and $[Ni_5(dpa)_4(NCS)_2]$ complexes, assuming the peak at 855.2 eV is from the low-spin configuration. This assumption is in qualitative agreement with the observations of structural analysis and magnetic behavior.

Conclusions

Detailed structural analyses and electronic properties of $[Ni_5(tpda)_4X_2]$ complexes are reported and discussed in this paper. The pentanuclear linear metal chain is helically wrapped by four *syn*−*syn*−*syn*−*syn* type ligands. The properties of the axial ligand and linearity between the Ni and the axial ligand both affect the bond distances of the terminal Ni−Ni bond. The magnetic susceptibility and X-ray near-edge absorption spectrum agree well with the model that two unpaired electrons are located at each of the two terminal Ni(II) ions and all the inner Ni ions have paired electronic configurations. The negative J value reveals an antiferromagnetic interaction of terminal high-spin nickel ions.

Acknowledgment. We thank the National Science Council of the Republic of China for financial support and Professor Yu Wang for stimulating discussion.

Supporting Information Available: Tables listing detailed crystal data and intensity collection parameters, fractional coordinates, atomic thermal parameters and fixed hydrogen coordinates, and bond distances and angles for compounds **1**−**5** and figures showing crystal structures for compounds **2**, **3**, and **5**, magnetic susceptibility measurements for compounds **3**−**5**, and a molecular orbital diagram for $[Ni_5(tpda)_4(NCS)_2]$ (48 pages). Ordering information is given on any current masthead page.

IC971608K

(29) van der Laan, G.; Thole, B. T.; Sawatzky, G. A. *Phys. Rev.* **1988**, *37*, 6587.
(30) van Elp, J.; Peng, G.; Searle, B. G.; Mitra-Kirtley, S.; Huang, Y. H.; Johnson, M. K.; Zhou, Z. H.; Adams, M. W. W.; Maroney, M. J.; Cramer, S. P. *J. Am. Chem. Soc.* **1994**, *116*, 1918.